E4F1: a novel candidate factor for mediating BMI1 function in primitive hematopoietic cells

Jalila Chagraoui,[1] Sherry L. Niessen,[1] Julie Lessard,[1] Simon Girard,[1] Philippe Coulombe,[2] Martin Sauvageau,[1] Sylvain Meloche,[2,3] and Guy Sauvageau[1,4,5]

[1]Laboratory of Molecular Genetics of Hematopoietic Stem Cells, Institut de Recherche en Immunologie et Cancérologie (IRIC), C.P. 6128 succursale Centre-Ville, Montréal, Québec H3C 3J7, Canada; [2]Laboratory of Signaling and Cell Growth, Institut de Recherche en Immunologie et Cancérologie (IRIC), C.P. 6128 succursale Centre-Ville, Montréal, Québec H3C 3J7, Canada; [3]Departments of Molecular Biology and Pharmacology, Université de Montréal, Montréal, Québec, Canada; [4]Department of Medicine, Division of Hematology, and Leukemia Cell Bank of Quebec, Maisonneuve-Rosemont Hospital, Montréal, Québec H1T, 2M4, Canada

The Polycomb group gene *Bmi1* is essential for the proliferation of neural and hematopoietic stem cells. Much remains to be learned about the pathways involved in the severe hematopoietic phenotype observed in *Bmi1* homozygous mutant mice except for the fact that loss of *p53* or concomitant loss of *p16^{Ink4a}* and *p19^{Arf}* functions achieves only a partial rescue. Here we report the identification of E4F1, an inhibitor of cellular proliferation, as a novel BMI1-interacting partner in hematopoietic cells. We provide evidence that *Bmi1* and *E4f1* genetically interact in the hematopoietic compartment to regulate cellular proliferation. Most importantly, we demonstrate that reduction of *E4f1* levels through RNA interference mediated knockdown is sufficient to rescue the clonogenic and repopulating ability of *Bmi1$^{-/-}$* hematopoietic cells up to 3 mo post-transplantation. Using cell lines and MEF, we also demonstrate that INK4A/ARF and p53 are not essential for functional interaction between *Bmi1* and *E4f1*. Together, these findings identify E4F1 as a key modulator of BMI1 activity in primitive hematopoietic cells.

The Polycomb group (PcG) proteins were initially identified in *Drosophila* as repressors of homeotic genes (Moehrle and Paro 1994). PcG proteins assemble into discrete chromatin-associated complexes that ensure the stable inheritance of gene expression state through cell division. The Polycomb repressive complex 1 (PRC1) includes BMI1, RING1/2, MEL-18, RAE28/MPH1, and M33/CBX2, while other complexes (PRC2/3/4) comprise, among other proteins, EED, EZH1/2, and SUZ12 (Valk-Lingbeek et al. 2004). Evidence that the molecular activity of PRC results in covalent modifications of both nucleosomal and nonnucleosomal histones is rapidly accumulating (Wang et al. 2004; Cao et al. 2005; Hernandez-Munoz et al. 2005). The SET domain proteins EZH1/2 are methyltransferases that specifically target lysine 27 in histone H3 (H3K27) and lysine 26 in histone H1 (H1K26). Trimethylation of H3K27 is required for recruitment of the BMI1-containing PRC1 complex, in which BMI1 represents an essential cofactor of the RING1/2 monoubiquitin E3 ligase implicated in the ubiquitination of histone H2A (Cao et al. 2005).

PcG genes regulate the activity of many different types of blood cells. These include the T- and B-cells whose maturation and/or proliferation is dependent on *Mel-18*, *Bmi1*, *Rae-28/Mph1*, and *M33/Cbx2* genes (Core et al. 1997; Tokimasa et al. 2001; Ohta et al. 2002; Lessard and Sauvageau 2003; Miyazaki et al. 2005). Hematopoietic stem cells (HSCs), which possess the unique property to generate all blood cell types and to self-renew, are also highly dependent on the activity of several PcG proteins. The role for BMI1 in HSC proliferation and self-renewal is best characterized. *Bmi1* expression is mostly detected in primitive human (CD34$^+$ CD45$^-$ CD71$^-$) and mouse (Sca1$^+$ Lin$^-$) bone marrow (BM) cells (Lessard et al. 1998; Lessard and Sauvageau 2003; Park et al. 2003). Nullizygosity for the *Bmi1* gene in mice leads to severe aplastic anemia presumably due to a progressive impairment of HSC self-renewal (van der Lugt et al. 1994; Lessard et al. 1999; Lessard and Sauvageau 2003; Park et al. 2003). Retroviral expression of *Bmi1* in *Bmi1$^{-/-}$* fetal liver (FL) cells

completely rescued the proliferative activity of myeloid progenitors to wild-type levels, indicating that this gene is dispensable for the generation of FL-derived myeloid progenitors but essential for their full proliferative activity (Lessard and Sauvageau 2003). In line with these results, complementation studies suggest that HSC numbers are normal (A. Faubert and G. Sauvageau, in prep.) in embryonic day 14.5 (E14.5) $Bmi1$-null FLs. Moreover, studies by Park and colleagues (Park et al. 2003) documented the inability of BM and FL-derived $Bmi1^{-/-}$ cells to sustain long-term production of blood cells in transplantation chimers, demonstrating a cell-autonomous impairment of their self-renewal potential.

The proliferative potential of $Bmi1^{-/-}$ hematopoietic progenitors is gradually lost from fetal to adult developmental stages, possibly indicating that these cells undergo a premature senescence (van der Lugt et al. 1994; Lessard et al. 1999; Lessard and Sauvageau 2003). Supporting this possibility, $Bmi1^{-/-}$ hematopoietic progenitors accumulate high levels of the senescence marker SA-β-gal (see Results) upon short-term proliferation. The senescent phenotype is also associated with increased levels of the tumor suppressor proteins p16^{INK4A} and p19^{ARF}, which are known to impair CDK4- and CDK6-induced phosphorylation of Rb and prevent the functional inactivation of p53 by binding to MDM2, respectively (Serrano et al. 1993; Quelle et al. 1995; Kamijo et al. 1998; Pomerantz et al. 1998; Weber et al. 1999). In the absence of $Bmi1$, primary mouse embryonic fibroblasts (MEFs) are impaired in progression into the S phase of the cell cycle and undergo premature senescence (Jacobs et al. 1999). In these fibroblasts and in $Bmi1$-deficient lymphocytes, the expression of the tumor suppressors $p16^{Ink4a}$ and $p19^{Arf}$ is raised markedly. Conversely, overexpression of $Bmi1$ in MEFs clearly down-regulates the expression of $p16^{Ink4a}$ and $p19^{Arf}$, delays replicative senescence, and facilitates immortalization (Jacobs et al. 1999). Similarly, overexpression of $Bmi1$ in primary human fibroblasts extended their replicative life span by suppressing the p16^{INK4A}-dependent senescence pathway (Itahana et al. 2003).

Iwama and collaborators (Iwama et al. 2004) showed that primitive (i.e., lineage-negative) $Bmi1^{-/-}$ E14.5 FL cells express high levels of $p16^{Ink4a}$ and $p19^{Arf}$ compared to wild-type controls, whereas only $p16^{Ink4a}$ levels were high in total (unpurified) FL cells. Although not investigated in primitive hematopoietic cells until recently, inactivation of the INK4A/ARF pathway marginally reduced the hematopoietic cell proliferation defects of $Bmi1$-null mutants (Bruggeman et al. 2005; Molofsky et al. 2005), indicating that INK4A/ARF is not the only critical in vivo downstream target for BMI1 in the regulation of HSC activity. In support to this, we reported that $Bmi1^{-/-}$ leukemia cell lines lacking expression of $p16^{Ink4a}$ and $p19^{Arf}$ depended on ectopic expression of $Bmi1$ for their ability to produce acute leukemia in vivo (Lessard and Sauvageau 2003).

Thus, the identification of factors that mediate BMI1 function in HSCs is of significant interest. In this study, we show that the inhibitor of cell proliferation E4F1 interacts physically and genetically with Bmi1 to regulate HSC activity.

Results

Identification of the BMI1-interacting protein E4F1

A yeast two-hybrid assay was employed using BMI1 as "bait" to screen a human fetal liver-derived cDNA library (enriched for primitive hematopoietic cells). From a total complexity of ~1 million cotransformants, 14 nonauxotrophic clones representing eight different genes were identified. One interesting clone corresponded to the last four C-terminal zinc finger domains (amino acids 346–783) (Fig. 1A) of the E1A-regulated transcription factor, E4F1 (Fig. 1B, sections 2 and 6). The interaction between BMI1 and E4F1 was further suggested using pull-down assays performed with in vitro translated proteins (Fig. 1C, lane 1). The interaction surface between BMI1 and E4F1 was mapped using the yeast two-hybrid system and involved the central Helix–Turn–Helix (HTH) domain of BMI1 and the last four C-terminal zinc fingers domains of E4F1 (Fig. 1D,E).

To determine whether BMI1 and E4F1 associate in vivo in mammalian cells, coimmunoprecipitations were carried out first using 293T cells transfected with HA-tagged E4F1. Western blot analysis of proteins coimmunoprecipitated with BMI1 confirmed the interaction between BMI1 and tagged E4F1 (Fig. 1F). We also analyzed the subcellular distribution of the complex; interestingly, we showed that the endogenous E4F1 (see asterisk in Fig. 1F, lane 2) as well as the tagged protein (Fig. 1F, lane 4) were complexed to BMI1 specifically in the cytoplasmic compartment (Fig. 1G). The subcellular localization of endogenous BMI1 and E4F1 was confirmed using confocal microscopy (data not shown).

Bmi1 interacts genetically with E4f1 in cell lines

To establish further the functional relationships between $Bmi1$ and $E4f1$, we first examined the impact of overexpressing $Bmi1$ and $E4f1$ on the proliferation of NIH 3T3 cells (Fig. 2A,B). While $E4f1$ and $Bmi1$ showed opposite effects on the proliferation rate of these cells, $Bmi1$ overexpression partially but consistently rescued the proliferative defect induced by $E4f1$. Moreover, we observed that the HTH domain of BMI1, through which E4F1 binds, is required to abrogate the proliferation defect associated with E4F1 (Fig. 2A), while the ΔPEST mutant, which still associates with E4F1, provides a rescue similar to that observed with wild-type BMI1 (data not shown).

Changes in proliferation rates were accompanied by modification of Rb phosphorylation status. Indeed, ectopic expression of $E4f1$ resulted in accumulation of the hypophosphorylated form of Rb (hypo-Rb), and reintroduction of $Bmi1$, but not the ΔHTH mutant, prevented this accumulation (Fig. 2C).

To further analyze the genetic interaction between

Figure 1. Identification of the BMI1 interacting protein E4F1. (*A*) Schematic representation of *E4f1* and the isolated clone C-*E4f1*. (*B*) BMI1 specifically associates with E4F1 in yeast. AH109 yeast were cotransfected with GAL4-DNA binding (pGBKT7) and GAL4-transactivation domain (pGADT7 or pACT2) expression vectors encoding *Bmi1*, *E4f1*, *Ring1b* (positive control), and Large T antigen or Lamin C (both negative controls). Interactions were monitored between (1) BMI1 and Large T, (2,6) BMI1 and C-E4F1, (3) BMI1 and GAL4 AD, (4) GAL4 alone (5) C-E4F1 and Lamin C, (7) C-E4F1 and GAL4 DB, and (8) BMI1 and RING1B (positive control). (*C*) Direct physical association between BMI1 and E4F1. In vitro transcribed–translated ^{35}S-labeled proteins were immunoprecipitated (IP) with an antibody specific to Bmi1 and separated by SDS-PAGE. (*D,E*) Interaction domain between BMI1 and E4F1 assessed in yeast. The correct folding of the *Bmi1* deletion mutants was ensured by demonstrating their potential to interact with RING1B and HPH1, proteins known to interact with the RING and HTH domains of BMI1, respectively. (*F*) BMI1 and E4F1 specifically coimmunoprecipitate in mammalian cells. 293T cells were transfected with HA-HOXB4 (negative control), HA-RING1B (positive control), or an HA-tagged version of the C-terminal E4F1 fragment clone isolated in the screen. Immunoprecipitations were performed overnight on total cellular extracts using an antibody specific to BMI1. Western blots were revealed using anti-HA antibody. (*G*) BMI1 and E4F1 associate in the cytoplasm. Nuclear (Nuc) and cytoplasmic (Cyto) extracts were generated from HA-E4F1 and control K562 cells. Extracts were immunoprecipitated with an antibody to BMI1, and associated proteins were revealed by Western blotting with antibodies to HA, E4F1, and BMI1. (*, lane 2) Endogenous E4F1.
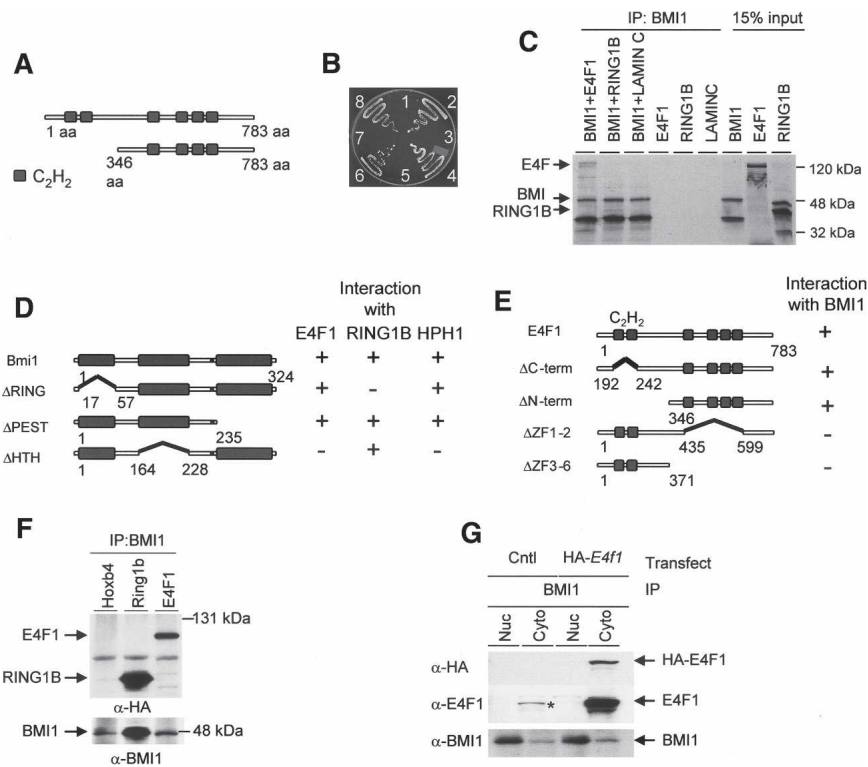
Bmi1 and *E4f1*, we generated shRNA vectors that efficiently suppressed *Bmi1* and *E4f1* expression (Fig. 2D). Knockdown of *Bmi1* severely impaired proliferation of NIH 3T3 cells, while the reduction of E4F1 protein levels enhanced cellular proliferation. Importantly, the proliferative defect induced by *Bmi1* knockdown was largely rescued by the reduction in E4F1 protein levels (Fig. 2E).

Bmi1/E4f1 *genetic interaction in the absence of* p19$^{\text{Arf}}$ *and* p53

Several experiments were performed to determine whether the $p19^{Arf}$–p53 axis is essential for E4F1-mediated effects. The proliferation-inhibitory effect of *E4f1* overexpression was first examined in various cell lines carrying defined genetic alterations in the $p19^{Arf}$ or/and *p53* genes. Results from these studies suggested that INK4A/ARF is not required for E4F1-induced proliferation defect, but a correlation was observed between the responses to *E4f1* overexpression and the *p53* status (Supplemental Table 1). We next studied the effect of E4F1 on proliferation of the *p53*-deficient K562 cells, which appeared to be refractory to E4F1-mediated proliferation arrest (Fig. 3A). Interestingly, reintroduction of *p53* inhibited expansion of these cells without restoring

the proliferation-inhibitory function of E4F1 (Fig. 3A), indicating either that additional factors or p53-confounding factors are involved.

To test this possibility further, the human papilloma virus *E6* gene was ectopically expressed in *E4f1*-overexpressing NIH 3T3 cells (*INK4A/ARF* locus deleted) to acutely induce p53 degradation, thereby changing their ability to proliferate (Fig. 3B). Interestingly, E6-transduced NIH 3T3 cells remained sensitive to E4F1-induced proliferation-inhibitory function (Fig. 3B). MEFs were then isolated from $p53^{-/-}$ mice and from littermate controls (e.g., $p53^{+/+}$), and the presence of *Bmi1–E4f1* genetic interaction was evaluated. The results presented in Figure 3C indicate that $p53^{-/-}$ MEFs show a reduction in BrdU incorporation in response to shRNA to *Bmi1* and a strong increase in response to *shE4f1*. Moreover, the genetic interaction between *E4f1* and *Bmi1* is conserved in these $p53^{-/-}$ cells. Importantly, MEFs from these experiments were also assessed for apoptosis by Annexin V and PI staining and, as observed in NIH 3T3 cells, no difference was detected between the various populations (data not shown).

We next tested the p53-mediated induction of p21 in irradiated NIH 3T3 cells engineered to express high levels of E4F1 (Fig. 3D) and found that p21 induction in
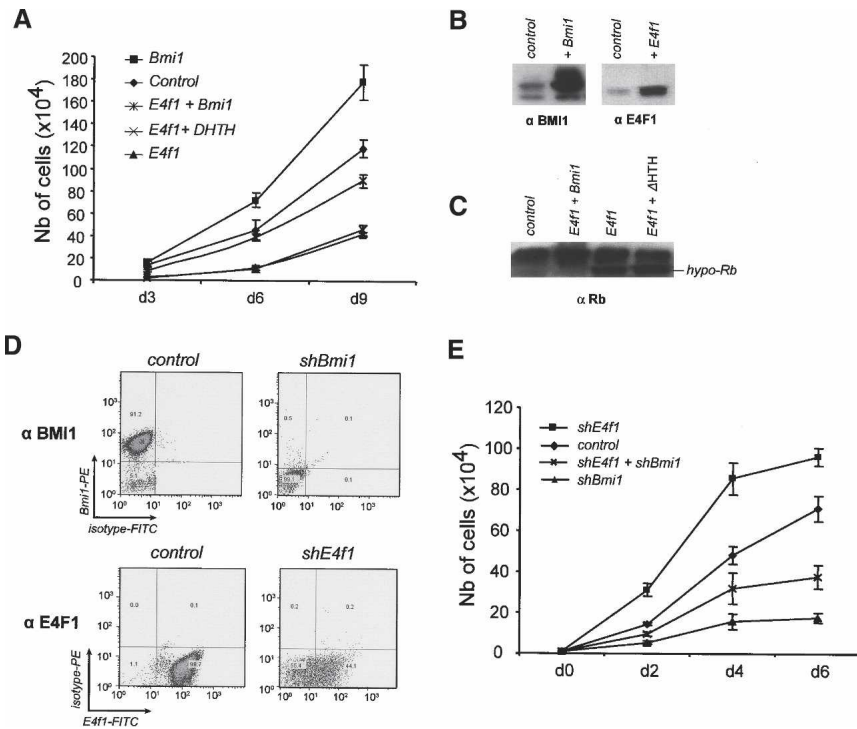
Figure 2. Genetic interaction between *Bmi1* and *E4f1* in NIH 3T3. (*A*) NIH 3T3 cells that express *E4f1* or *Bmi1*, or coexpress *E4f1* and *Bmi1* were plated in triplicate, and counted at the indicated time points. Cells were collected at day 9 and analyzed by Western blot for the expression of (*B*) BMI1 and E4F1 or (*C*) Rb protein (hypo-Rb:hypophosphorylated Rb). (*D*) NIH 3T3 cells infected with retroviruses encoding *shBmi1*, *shE4f1*, or an empty vector were fixed, permeabilized, and stained sequentially with primary antibodies (mouse anti-BMI1 and rabbit anti-E4F1) and the matched conjugated secondary antibodies (anti-mouse PE and anti-rabbit FITC) and then analyzed by flow cytometry. (*E*) Proliferation of NIH 3T3 cells infected with retrovirus encoding *shBmi1*, *shE4f1*, or both. For *A* and *E*, proliferation was measured in three independent experiments each resulting from newly infected and selected cellular populations assessed in duplicates within 6 d of infection. Data are given as means ± SD. Populations assessed in these experiments are polyclonal.

response to γ-rays was not altered by *E4f1* overexpression.

Together, these results strongly suggest that p16^{INK4A}/p19^{ARF} and p53 are not required, at least separately, for the *E4f1/Bmi1* genetic interaction.

E4f1 knockdown rescues Bmi1$^{-/-}$ hematopoietic cells without affecting p16^{Inka} and p19^{Arf} expression

We next tested whether *Bmi1* and *E4f1* also interact genetically in primitive hematopoietic cells. Real-time Quantitative-PCR analysis demonstrated the coexpression of these two genes in the stem-cell-enriched subpopulations (KLS CD34$^-$ and KLS CD34$^+$) and confirmed the preferential expression of *Bmi1* mRNA in cells with long-term repopulating activity (KLS CD34$^-$) (Fig. 4A).

Flow cytometry analysis of E4F1 protein levels in fetal liver cells isolated from *Bmi1*$^{-/-}$ or wild-type embryos revealed that a subpopulation of *Bmi1*$^{-/-}$ cells expresses higher levels of E4F1 than populations of wild-type cells (Fig. 4B). Consistent with the high levels of *Bmi1* expression in Sca1-positive cells, we found that the accumulation of E4F1 occurs within the Sca1$^+$ population of *Bmi1*$^{-/-}$ cells (Fig. 4C).

Based on these observations and to further address the role of E4F1 in BMI1-mediated HSCs proliferation, we examined whether *E4f1* silencing could rescue the hematopoietic defect induced by loss of *Bmi1*.

To test this possibility, fetal liver cells were isolated from *Bmi1*$^{-/-}$ or wild-type embryos and infected with *shE4f1*, *Bmi1*, or *GFP* (control) retroviruses as described in Figure 5A. Cultures initiated with wild-type (*Bmi1*$^{+/+}$) cells infected with the control *GFP* vector generated nu-

merous small and round cells with birefringent properties (Fig. 5B). In sharp contrast, *Bmi1*$^{-/-}$ cells infected with the control vector rapidly (by day 4) gave rise to poorly proliferating cultures that contained a majority of flat, granulous, and nonbirefringent cells (Fig. 5B). Qualitatively, the proliferation and morphological properties typical of *Bmi1*$^{-/-}$ cells were completely rescued by reducing the levels of *E4f1* by RNA interference (Fig. 5B).

In agreement with these results, BrdU incorporation experiments indicated that while absence of *Bmi1* resulted in a dramatic decrease in DNA synthesis (only 2.1% BrdU$^+$ cells after 6 d of culture) and G$_1$-phase accumulation (data not shown), reduction in E4F1 levels provided a rescue in DNA synthesis to levels comparable to those observed in wild-type cells (Fig. 5C). In agreement with findings in NIH 3T3 cells, increasing levels of BMI1 resulted in enhanced BrdU incorporation (Fig. 5C). In addition, as shown by annexin V and propidium iodide staining, there was no significant difference in the proportion of cells undergoing apoptosis between wild-type or *Bmi1*$^{-/-}$-derived cells (Fig. 5D), precluding a possible apoptotic effect of *Bmi1* loss.

Since *Bmi1* deletion in MEF induced a premature senescence phenotype associated with INK4A/ARF derepression, we asked whether *Bmi1*$^{-/-}$-derived hematopoietic cells also undergo cellular senescence as a consequence of *p16*^{Ink4a} and *p19*^{Arf} up-regulation. Therefore, cultures initiated with *Bmi1*$^{-/-}$ cells were stained for senescence-associated β-galactosidase (SA-β-gal) activity, a well-established biomarker for senescent cells. While SA-β-gal activity is nearly undetectable in *Bmi1*$^{+/+}$-derived cultures (<5% positive cells) (data not shown), the percentage of SA-β-gal$^+$ cells reached 70%–80% in cul-
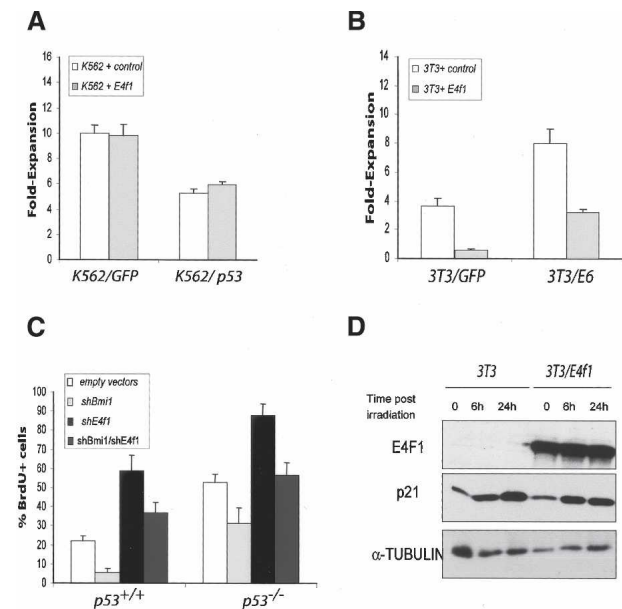
Figure 3. p19^{Arf}/p53 is not required in *Bmi1–E4f1* interaction. (*A*) K562 cells (INK4A/ARF$^{-/-}$/p53$^{-/-}$) were sequentially transduced with MSCV-*p53-GFP* (or appropriate empty vector) and *MSCV-Neo-E4f1* (or corresponding empty vector). Cells were kept in G418-containing medium during 7 d and then plated in triplicate and counted 4 d later. Relative cell expansions were measured in two independent experiments each resulting from newly infected and selected cellular populations assessed in triplicates within 6 d of infection. Data are given as means ± SD. (*B*) NIH 3T3 cells (INK4A/ARF$^{-/-}$/p53$^+$) were sequentially transduced with *MSCV-E6- GFP* (or appropriate empty vector) and *MSCV-Neo-E4f1* (or corresponding empty vector). Cells were kept in selective medium (containing G418 to prevent loss of *E4f1* expressing retrovirus) during 7 d and then plated in triplicate and counted 4 d later. Relative proliferation rates were determined from two triplicate experiments (two independent infections). (*C*) BrdU incorporation assay in primary mouse embryonic fibroblasts (MEF) derived from p53$^{+/+}$ or p53$^{-/-}$ E14.5 embryos and infected with combinations of control, *shBmi1*, and *shE4f1* retroviruses. Cells were infected on day 3, and the BrdU pulse was 10 h. BrdU incorporation on day 6 after infection was measured in two independent experiments each resulting from newly infected and selected cellular populations assessed in triplicates within 6 d of infection. Data are given as means ± SD. (*D*) Whole cell protein extracts were prepared from control or *E4f1*-transduced NIH 3T3 cells at different time intervals (in hours) after exposure to a 5-Gy dose of ionizing radiation prior to Western blot analysis for E4F1, p21, and α-TUBULIN (loading control).

tures initiated with *GFP*-transduced *Bmi1*$^{-/-}$ cells by day 7 (Fig. 5E, upper right panel). As described in previous work, we found that p16^{INK4A} and p19^{ARF} protein levels were significantly greater in *GFP*-transduced *Bmi1*$^{-/-}$ cells than in *GFP*-transduced wild-type cells (Fig. 5E, histogram overlay showing 16^{INK4A} and p19^{ARF} levels, upper panels). The expression of mRNA levels for *p16*^{Ink4a} and *p19*^{Arf} in *Bmi1*$^{-/-}$ cells was also determined by quantitative RT-PCR (Q-PCR) and confirmed that *p16*^{Ink4a} and, to a lesser extent, *p19*^{Arf} mRNA levels were up-

regulated on average 50-fold and 20-fold compared to control wild-type cells after 7 d of culture, respectively (data not shown).

As expected, the reintroduction of *Bmi1* in *Bmi1*$^{-/-}$ cells led to a nearly complete bypass of the senescence as determined by the decrease in the proportion of cells exhibiting SA-β-gal activity (10%–20% SA-β-gal$^+$ cells) and down-regulation of p16^{INK4A} and p19^{ARF} proteins (Fig. 5E, middle panels) and mRNA (15-fold and 10-fold reduction) levels (data not shown).

Interestingly, *Bmi1*$^{-/-}$ cells engineered to express low E4F1 levels also escape (partially) senescence (30%–40% SA-β-gal$^+$ cells) but without affecting p16^{INK4A} or p19^{ARF} protein (Fig. 5E, lower panels) and mRNA levels (data not shown).

Reduction in E4F1 levels rescues proliferative defects of Bmi1$^{-/-}$ stem and progenitor cells

The in vitro and in vivo maintenance of progenitor and stem cell activity depends on the presence of *Bmi1* (Lessard and Sauvageau 2003; Park et al. 2003). To determine whether *Bmi1*$^{-/-}$ hematopoietic progenitor cells engineered to express low E4F1 levels could be recovered following in vitro cultures, we monitored colony-forming cell (CFC) activity at different time in cultures as indicated in Figure 5A. While at initiation of cultures (i.e., day 0) CFC activity was similar in all groups, their numbers increased steadily for 6 d in cultures initiated with either wild-type cells or with mutant cells engineered to express high levels of BMI1 (Fig. 5F). As expected, no progenitor activity could be recovered from cultures initiated with *Bmi1*$^{-/-}$ cells transduced with *GFP*, but normal CFC activity was detected for *Bmi1*$^{-/-}$ cells in which levels of E4F1 were reduced (e.g., Fig. 5F, cf. bars and asterisk). These data indicate that *E4f1* knockdown in *Bmi1*-deficient cells resulted in a complete rescue of their clonogenic activity. Importantly, *E4f1* knockdown in wild-type cells had no effect on their capacity to generate CFCs, demonstrating the specificity of the reported effect (Fig. 5F).

In selected experiments, a competitive proliferation assay was set up by adjusting the proportion of transduced cells (GFP$^+$) to 50% at initiation of the cultures. The evaluation of transduced CFCs along the culture showed that while wild-type cells transduced with *GFP* or *shE4f1-GFP* had no proliferative advantage over nontransduced cells, *Bmi1-GFP*-overexpressing cells expanded much better and became rapidly the predominant population of the culture (data not shown). Furthermore, after 4 d of culture, >95% of CFCs generated from *shE4f1*- or *Bmi1*-transduced *Bmi1*$^{-/-}$ cells were derived from transduced cells (i.e., GFP$^+$), indicating a cell-autonomous nature for the rescue induced by *E4f1* knockdown or *Bmi1* complementation (data not shown).

In addition to severe proliferation defects, *Bmi1*$^{-/-}$ progenitors maintained ex vivo for a short period of time became restricted in their differentiation potential to the monocyte/macrophage lineage. Reduction in E4F1 levels in these cells rescued their capacity for differentiation
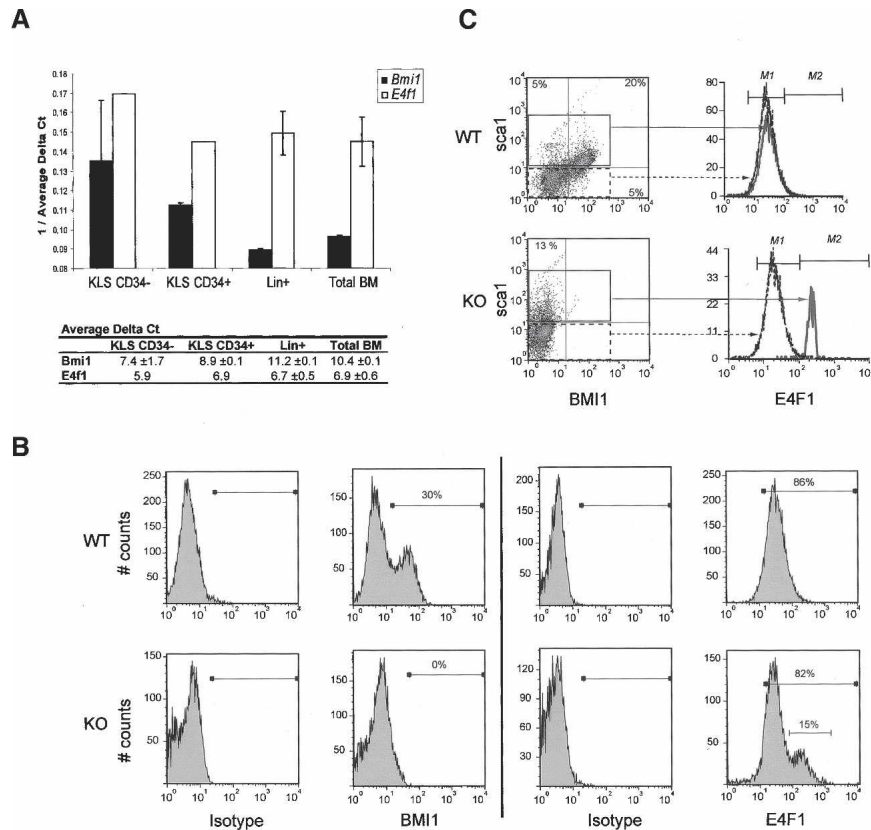
Figure 4. Expression of *E4f1* and *Bmi1* in primitive hematopoietic cells. (*A*) Quantitative RT-PCR of *Bmi1* and *E4f1* in bone marrow (BM) hematopoietic cells: For each sorted cell population, mRNA levels were determined by calculating the ΔCt values where the levels of mRNA for *Bmi1* and *E4f1* are normalized according to the endogenous control gene *Gapdh* ($\Delta Ct = Ct_{\text{target}} - Ct_{\text{endogenous control}}$). The graph shows ratios of $1/\Delta Ct$. ΔCt values are shown in the table *below*. Experiments were repeated twice with bone marrow cells extracted from two series of >150 animals. Each Q-PCR reaction was performed in duplicate using automated pipette delivery systems (Biomek FX; Beckman). (*B*) *Bmi1*^{+/+} and *Bmi1*^{−/−} fetal liver cells were cultured for 2 d, fixed, permeabilized, and analyzed by flow cytometry for BMI1 or E4F1 expression levels. (*C*) *Bmi1*^{+/+} and *Bmi1*^{−/−} fetal liver cells were simultaneously stained with anti-Sca1, anti-BMI1, and anti-E4F1 antibodies. The histogram overlay showed E4F1 expression levels in the Sca1-negative population (hatched line) and the Sca1-positive population (red line). For *B* and *C*, FACS profiles are representatives from more than three independent experiments.

since no significant change in the proportion (or size) of multipotent (i.e., CFU-GEMM) or bipotent and unipotent (i.e., CFU-GM, CFU-G, or CFU-M) colonies was detected in 4-d cultures initiated with wild-type versus *shE4f1*-transduced *Bmi1*^{−/−} cells (Fig. 5G, left panel). Furthermore, the phenotypic characterization performed by flow cytometry confirmed the presence of primitive cells (Lin[−] Sca1^{+}) and mature cells (Gr1^{+} or Mac1^{+}) in the cultures derived from *shE4f1*-transduced cells (data not shown). In addition, examination of the Wright-stained cytospin preparations of cells recovered from these cultures (Fig. 5G, right panel) showed that only macrophages persisted in cultures derived from the control *GFP*-transduced *Bmi1*^{−/−} cells, and that reduction of E4F1 protein levels in these cells enabled production of a variety of progenitors and differentiated cells.

Based on these observations, we presumed that the proliferative impairment of *Bmi1*^{−/−} repopulating cells might be rescued by reducing E4F1 levels. To test this possibility, a series of recipients that received *Bmi1*^{−/−} fetal liver cells transduced with *shE4f1-GFP* or with control *GFP* was generated. At multiple time points after transplantation, the recipients were analyzed for the presence of transduced donor cells (GFP^{+} cells) (Fig. 6A). In agreement with previous data, no donor-derived cells were detected in eight of eight recipients transplanted with *GFP*-transduced *Bmi1*^{−/−} cells.

Interestingly, while *E4f1* knockdown in wild-type cells does not lead to any detectable perturbation of hematopoietic repopulating ability, *shE4f1*-transduced *Bmi1*^{−/−} cells showed an increased contribution to peripheral blood in the recipients tested, providing evidence for a strong genetic interaction between *Bmi1* and *E4f1* in vivo for cells with repopulation potential lasting up to 12 wk (Fig. 6A).

To determine whether engrafted *shE4f1-GFP*-transduced *Bmi1*^{−/−} cells also retained their full differentiation ability, peripheral blood cells were stained at 12 wk post-transplantation for surface markers B220 (B-cell lineage), CD3 (T-cell lineage), Mac1 and Gr1 (myeloid lineage), in combination with the GFP marker. The presence of double-positive cells for GFP and each of these markers demonstrated the full potential of *Bmi1*^{−/−} cells engineered to express low E4F1 levels to differentiate into B lymphoid (B220+), T lymphoid (CD3+), and myeloid cells (Mac1+ or Gr1+) (see Fig. 6B).

Although *shE4f1* provides a good rescue of *Bmi1*^{−/−} cells with repopulation activity lasting at least 12 wk, it is important to analyze recipient mice at longer time points (e.g., >12–16 wk) because there is now clear evidence that at least two distinct and prospectively "isolable" populations of HSCs—termed short-term repopulating (STR) and long-term repopulating (LTR) HSCs—are present in the mouse bone marrow (Zhao et al. 2000; Benveniste et al. 2003). When analyzed at 22 wk post-transplantation, the persistence of *shE4f1*-transduced *Bmi1*^{−/−} cells was observed at low level (i.e., 3% ± 1%) in the peripheral blood of three recipients out of four (Fig. 6C), indicating that STR-HSCs are rescued by *shE4f1* but LTR-HSCs are not.

Figure 5. Loss of *E4f1* rescues the proliferative defect of *Bmi1* $^{-/-}$ hematopoietic progenitors. (*A*) Overview of the experimental strategy: *Bmi1*$^{+/+}$ and *Bmi1*$^{-/-}$ fetal liver cells (the equivalent of one fetal liver) were infected for 2 d with *GFP*, *Bmi1-GFP*, or *shE4f1-GFP* retroviruses (at an efficiency of 80%–92%). The equivalent of one-half fetal liver was kept in culture for 10 d and assayed at different time points for their content in colony-forming cells (CFC). The equivalent of one-half fetal liver was transplanted in irradiated mice for in vivo study (see Fig. 6). (*B*) *Bmi1*$^{+/+}$ and *Bmi1*$^{-/-}$ fetal liver cells engineered to express *GFP* or *shE4f1-GFP* retroviruses were visualized at day 4 of the culture under phase contrast microscopy (original magnification 20×). Representative of three independent experiments each with different fetal livers and retroviral preparations. (*C*) BrdU incorporation assay in primary FL cells. Cells were pulsed with BrdU for 24 h on day 4 after infection, and incorporation was measured in three independent experiments each resulting from newly infected cellular populations assessed in duplicates. Data are given as means ± SD. (*D*) The proportion of apoptotic cells was monitored by annexin V/PI staining. Representative of four independent experiments. (*E*) *Bmi1*$^{-/-}$ fetal liver cells engineered to express *GFP*, *Bmi1-GFP*, and *shE4f1-GFP* were assayed for senescence phenotype at day 6 of culture: The *left* panel showed representative flow cytometry analysis of p16^{Ink4a} and p19^{Arf}

expression in transduced *Bmi1*$^{-/-}$ cells (gray-filled histograms) compared to *GFP*-transduced wild-type cells (dotted line histogram), and the *right* panel shows a representative SA-β-gal staining of transduced *Bmi1*$^{-/-}$ cells. Representative of two independent experiments each performed in triplicate. (*F*) *Bmi1*$^{+/+}$ and *Bmi1*$^{-/-}$ fetal liver cells engineered to express *GFP* (ct, control), *Bmi1-GFP*, and *shE4f1-GFP* were assayed for their content in colony-forming cells (CFC) at different time of the culture. Results show means ± SD of four independent experiments performed in duplicate. (*G*) Frequency of colony type was evaluated after 4 d of culture by morphological (in toto) analysis and Wright staining of representative colonies. Representative of four independent experiments performed in duplicate.
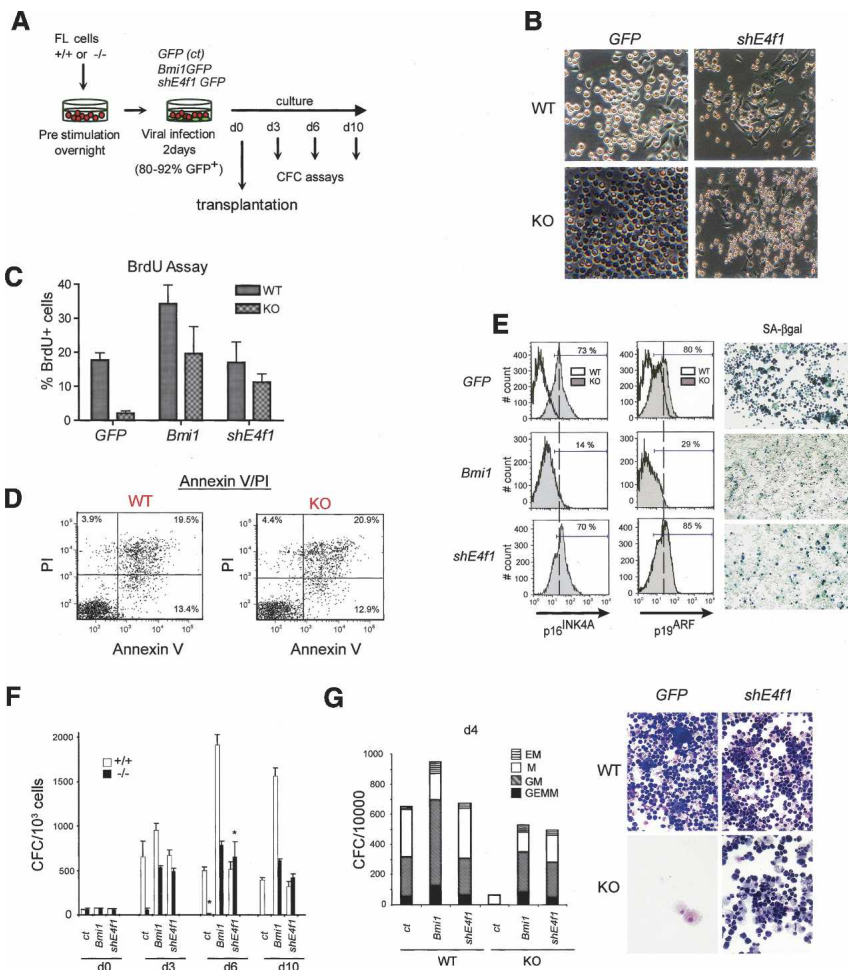
Interestingly the ΔHTH mutant of BMI1 (lacking interaction with E4F1) failed to restore both the short-term and long-term repopulating capacity of *Bmi1*$^{-/-}$ cells, while excellent rescue was observed with wild-type BMI1 and the PEST deletion mutant, which preserves E4F1 interaction (Fig. 6C).

Discussion

In this study, we have identified E4F1 as a new binding partner of BMI1 and provide comprehensive evidence that this protein functionally interacts with BMI1 to regulate cell proliferation. This conclusion is supported by several lines of evidence: Firstly, we show that BMI1 and E4F1 interact physically and genetically both in cell lines (e.g., NIH 3T3) and in primary cells (MEF and hematopoietic cells) to control cell proliferation. Secondly, our data suggest that the physical interaction between

these two proteins is important for this genetic interaction since the removal of the E4F1-interacting domain of Bmi1 eliminates its ability to rescue the proliferative defect induced by E4F1. Moreover, we provide evidence that *INK4A/ARF* and *p53* are independently not required for the genetic interaction between *E4f1* and *Bmi1* in selected cell lines and in MEFs. Finally and most importantly, the loss of E4F1 function in *Bmi1*$^{-/-}$ hematopoietic cells leads to the rescue of their clonogenic and repopulating ability without affecting levels of *p19*^{Arf} or *p16*^{Ink4a}, thus indicating that the effects of *E4f1* knockdown are not mediated through down-regulation of these CDK inhibitors.

Interestingly, the interaction between BMI1 and E4F1 appears to be restricted to the cytoplasm of dividing cells (J. Chagraoui, unpubl.), possibly revealing an unsuspected cytoplasmic and cell-cycle-dependent function for Bmi1. This observation is consistent with previous
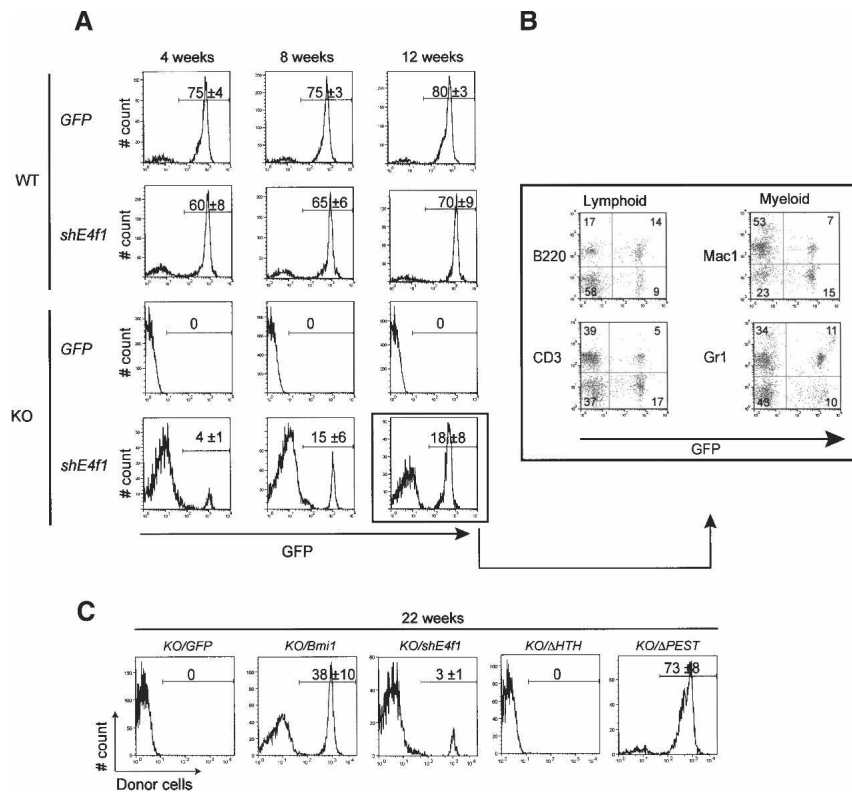
Figure 6. Loss of *E4f1* rescues the repopulating ability of *Bmi1*-deficient cells. (*A*) Two days after infection, *Bmi1*$^{+/+}$ and *Bmi1*$^{-/-}$ fetal liver (the equivalent of one-half fetal liver) cells (Ly5.2) engineered to express *GFP*, *Bmi1-GFP*, or *shE4f1-GFP* were injected into lethally irradiated congenic (i.e., Ly5.1) recipient mice along with Ly5.1 competitor cells. Repopulation activity of the transduced cells was evaluated by monitoring donor cell chimerism (Ly5.2$^+$ GFP$^+$) in peripheral blood 4, 8, and 12 wk after transplantation. The figure shows representative FACS profiles from four recipients per group and *n* = 2 independent experiments (mean values for repopulation ±SD are indicated). (*B*) Proportions of shE4f1-GFP transduced *Bmi1*$^{-/-}$ cells in myeloid (Mac-1 and Gr1) and lymphoid (B220 and CD3) populations were determined at 12 wk post-transplantation. The data shown are representative FACS profiles from one recipient. Note that lympho-myeloid reconstitution was confirmed in all four mice analyzed (see *A*). (*C*) Representative FACS profile showing donor contribution (GFP$^+$ Ly5.2$^+$) at 22 wk post-transplantation in the peripheral blood of recipients of *Bmi1*$^{-/-}$ fetal liver cells engineered to express *Bmi1-GFP*, *shE4f1-GFP*, or *Bmi1* mutants (ΔHTH-GFP and ΔPEST-GFP). Note that recipients for shE4f1 transduced cells are the same as used in *A* and *B*. Values are means ± SD of six recipients per group (for Bmi1 and the indicated mutants).

data showing a dissociation of BMI1 from the chromatin during mitosis (Voncken et al. 1999; Voncken et al. 2005). Other emerging evidence also supports a role for PcG proteins in various cellular processes apart from chromatin modification. For example, EZH2 associates with VAV1 specifically in the cytoplasm and thus contributes in the control of actin polymerization and cellular proliferation (Nolz et al. 2005; Su et al. 2005). These findings raise the interesting prospect of two dynamic processes (an epigenetic and a nonepigenetic) involving BMI1 and will require further investigations. In regard to these observations, one possibility is that BMI1 might sequester E4F1 or induce its degradation, thus counteracting its activity. This hypothesis, corroborated with the elevated E4F1 protein levels observed in the stem-cell-enriched subpopulation (i.e., Sca1$^+$) of *Bmi1*$^{-/-}$-deficient fetal liver cells, is further enforced by the new key role attributed to BMI1 and its PcG partner RING1A in H2A ubiquitination as well as in their own ubiquitination (Cao et al. 2005; Buchwald et al. 2006).

Surprisingly, and although the literature points out p19^{ARF}/p53 and p16^{INK4A}/Rb as being the major effector pathways for E4F1 function, we found that *p16*$^{Ink4a-/-}$ and *p19*$^{Arf-/-}$ cell lines (NIH 3T3, U2OS) still undergo a cell cycle arrest on *E4f1* overexpression. In addition, the proliferative rescue obtained in *Bmi1*$^{-/-}$ hematopoietic cells engineered to express a low level of E4F1 protein occurs without affecting *p16*^{Ink4a} and *p19*^{Arf} expression.

We also showed that the ability of p53 to induce p21 in response to irradiation is not affected by *E4f1* overexpression. Intriguingly, we did not observe a dramatic induction of p21 under *E4f1* overexpression as it has been shown by Fernandes et al. (1998), although E4F1 protein levels appear higher in our *E4f1*-transduced NIH 3T3 cells than in the 3T3/*E4f1* clone 7 (sent to us by Dr. R.J. Rooney and used as control) (data not shown). Moreover, in this clone 7, we did not observe further induction of p21 after irradiation, suggesting a selective rather than a direct impact of E4F1 on *p21* expression. Moreover, we show that *p53* deletion does not prevent the genetic interaction between *E4f1* and *Bmi1* in primary fibroblasts, although less pronounced than in wild type, indicating that p53 is not essential for the reported *Bmi1/E4f1* genetic interaction. These data are further substantiated by the observation that *p21*$^{-/-}$ and *p53*$^{-/-}$ fibroblasts overexpressing *E4f1* are still blocked in G$_1$ phase (Fajas et al. 2000).

The conclusion that BMI1/E4F1 interplay occurs independently of *INK4A/ARF* and possibly p53 in selected cell lines does not exclude an important role for these genes in complementing the hematopoietic defects of *Bmi1*-deficient mice. Indeed, previous studies indicated that complete deletion of the *INK4A/ARF* locus and the disruption of the *p53* gene in *Bmi1* mutant mice lead to a partial rescue of the hematopoietic defects (Bruggeman et al. 2005). It will thus be critical to investigate the genetic interaction between *E4f1, INK4A/ARF*, and *p53*

in primitive hematopoietic cells. Such experiments will require the generation of *E4f1* conditional alleles. The inability of our *E4f1* shRNA vector to confer a major rescue at 22 wk post-transplantation suggests that this gene is critical for the STR-HSCs and that LTR-HSCs may be rescued by inactivation of *INK4A/ARF* or *p53*. Therefore, the molecular events downstream from BMI1 appear to be more complex than expected, and several plausible mechanisms might be involved: First, BMI1 represses *INK4A/ARF* transcription through a mechanism that remains to be fully characterized. Second, BMI1 may inhibit E4F1 activity (ubiquitination?) on several cell-cycle-regulating proteins, including the CDK inhibitor p27^{KIP1}, CYCLIN E, and CYCLIN B1, with reduced CDK2, CDK4/6, and CDC2 kinase activities and with the down-regulation of *Cyclin A2* gene expression (Fernandes et al. 1998; Fajas et al. 2001; Rooney 2001). Moreover, HMGA2 protein, which plays an important role in chromatin organization, interacts with E4F1 and prevents its binding to the C*yclin A* promoter (Tessari et al. 2003). Finally, E4F1 may participate in the mitotic spindle checkpoint by interacting with the tumor suppressor RASSF1A, known to control microtubule stability and cell cycle progression (Fenton et al. 2004; Ahmed-Choudhury et al. 2005). Consistent with these data, *E4f1* is essential for embryonic development and cell division, as *E4f1*-deficient mouse embryos die at preimplantation stages and *E4f1$^{-/-}$* blastocysts display several mitotic abnormalities and chromosomal missegregation (Le Cam et al. 2004). These observations are most interesting since one of the eight BMI1-interacting proteins identified in our yeast two-hybrid screen physically localizes to the centrosome and interacts with RASSF1A. It is thus conceivable that BMI1 may alter the interaction between E4F1 and microtubule-associated proteins to ensure normal chromosome segregation and cell cycle progression.

Together these observations suggest that BMI1 creates a complex but effective network for the control of cell proliferation and senescence and might orchestrate multiple pathways that cooperatively mediate E4F1 and INK4A/ARF function on the proliferation of stem and progenitor cells. Most interestingly, the analysis of the genes involved may clarify the molecular bases that underlie STR-HSCs versus LTR-HSCs.

Materials and methods

Yeast two-hybrid screen

A yeast two-hybrid screen was performed according to Clontech protocol using *Bmi1* as bait to screen a human fetal liver cDNA library. Two rounds of screening yielded 14 positive clones corresponding to eight different cDNA sequences, all of which interacted specifically with BMI1 but not with control baits (Large T antigen, LaminC). One of these cDNAs contained a 1.6-kb partial cDNA corresponding to *E4f1*.

Western blotting and immunoprecipitations

Preparation of total, nuclear, and cytoplasmic extracts was done as described (Borden et al. 1998). Immunoprecipitations and immunoblots were done according to published methods.

Quantitative RT-PCR

The quantification of *Bmi1* and *E4f1* gene expression was performed in two independent experiments by real-time PCR on an ABI Prism 7900HT Sequence Detection System according to the manufacturer's recommendation. Briefly, KLS (Kit$^+$ Lin$^-$ Sca1$^+$) CD34$^-$, KLS CD34$^+$, and LIN$^+$ (B220$^+$; TER119$^+$; GR1$^+$) subpopulations were sorted from two separate pools of mice bone marrow cells, and total RNA was harvested. For the total bone marrow (BM) sample, RNA was directly harvested from an aliquot of those pools. cDNA was generated using random primers and MMLV RT (Invitrogen) according to the manufacturer's protocol. Q-PCR reactions were carried out in a total volume of 10 µL on 25–50 ng of cDNA using TaqMan Universal Master Mix (Applied Biosystems) and Universal ProbeLibrary assays designed with the ProbeFinder software (Roche Applied Science). The primer sequences and Universal Probe numbers used are available upon request. ABI Prism 7900HT SDS was programmed to an initial step of 2 min at 50°C and 10 min at 95°C, followed by 40 cycles of 15 sec at 95°C and 1 min at 60°C. All reactions were run in duplicate, and the average values were used for quantification. The mouse *Gapdh* predeveloped TaqMan assay was used as the endogenous control to normalize expression values of *Bmi1* and *E4f1* ($\Delta CT = Ct_{target} - Ct_{Gapdh}$).

For p19^{Ink4a} and p16^{Arf} gene expression, total RNA was isolated by Trizol and DNase-I-treated, and cDNA was prepared according to the manufacturer's instructions (Invitrogen). Q-PCR reactions were carried out using TaqMan probe-based chemistry (Applera). The primer and probe sequences are as follows: p16^{Ink4a}, forward, 5′-CCCAACGCCCCGAACT-3′, reverse, 5′-CGTGAACGTTGCCCATCA-3′ and 5′-FAM-TCG GTCGTACCCCGATTCAGGTGAT-TAMRA-3′; p19^{Arf}, forward, 5′-GGGCCGCACCGGAAT-3′, reverse, 5′-AGCAGAA GAGCTGCTACGTGAA-3′ and 5′-FAM-CTGGACCAGGT GATGATGATGGGCAAC-TAMRA-3′. The 18S rRNA Taqman assay (ABI) was used as the endogenous control gene. Relative fold differences were determine by the $\Delta\Delta Ct$ method using the wild-type fetal liver cells transduced with control *GFP* vector as the calibrator sample.

Generation of shRNA

Five short hairpin RNA (shRNA) sequences specific to *E4f1* were designed and cloned in a retrovirus containing the RNA polymerase III promoter. Only one shRNA (5′-AAGATTCA GAAGACCTGCCAT-3′) represses *E4f1* efficiently. The *shBmi1* encoding retrovirus was a gift from Martin Von Lohuizen (The Netherlands Cancer Institute).

Mice genotyping

Bmi1 mutant mice were genotyped by Southern blot analyses as described (van der Lugt et al. 1994). p53 mutant mice (Jackson Laboratory, Maine) were genotyped by PCR according to the manufacturer's instructions (Jax Mice Web site, http://jaxmice. jax.org).

In vitro clonogenic progenitor assays

For myeloid clonogenic progenitor assays, cells were plated in 35-mm dishes in semisolid medium, containing 1% methylcellulose in α medium supplemented with 10% fetal calf serum (FCS), 5.7% bovine serum albumin, 10^{-5} β-mercaptoethanol (β-ME), 1 U/mL erythropoietin (Epo), IL-3, IL-6, Steel, 2 mM glutamine, and 200 mg/mL transferrin. Colonies were scored on day 7 of incubation as derived from CFU-GM, BFU-E, or CFU-GEMM according to standard criteria. For some of the experi-

ments, identification of the colony types was confirmed by Wright staining of cytospins preparations of colonies.

Retroviral generation, infection, and transplantation of E14.5 fetal liver and bone marrow cells

Details of the different retroviral vectors used in this study are available on request. Production of vesicular stomatitis virus-pseudotyped (VSV) retroviruses, infection of hematopoietic cells, and transplantation into mice were done as described (Thorsteinsdottir et al. 2002).

Flow cytometry

Flow cytometry analyses were performed using a LSRII cytometer (Becton Dickinson). For intracellular antigens, cells were first fixed with 3.7% paraformaldehyde and permeabilized with 0.25% Triton X-100. BMI1 and E4F1 were revealed using primary antibodies (monoclonal anti-Bmi1 antibody [Clone F6, Upstate] and polyclonal rabbit anti-E4F1 antibody [provided by R.J. Rooney], respectively) and secondary antibodies (goat anti-mouse PE, goat anti-rabbit FITC).

Cell cycle and apoptosis analyses

Analysis of BrdU incorporation was performed using the BrdU Flow Kit (PharMingen) in accordance with the manufacturer's instructions. Cell cycle analysis was performed after ethanol fixation, RNase digestion, and propidium iodide staining using BD ModFit LT software. Cultured cells from $Bmi1^{-/-}$ or $Bmi1^{+/+}$ fetal livers were stained with FITC-annexin V (Becton Dickinson) and propidium iodide (50 µg/mL) in accordance with the manufacturer's instructions, and analyzed by flow cytometry.

Senescence analyses

SA-β-galactosidase activity was determined using a SA-β-gal staining kit from Cell Signaling Technology according to the manufacturer's instructions. Briefly, hematopoietic cells harvested from 7-d fetal liver cultures were seeded onto polylysine-coated slides. Cells were fixed in 2% (v/v) formaldehyde and 0.2% glutaraldehyde, and then incubated in SA-β-gal staining solution (1 mg/mL 5-bromo-4-chloro-3-indolyl β-D-galactosidase; 40 mM citric acid at pH 6.0, 40 mM sodium phosphate at pH 6.0, 5 mM potassium ferrocyanide, 5 mM potassium ferricyanide, 150 mM sodium chloride, and 2 mM magnesium chloride) at 37°C for 10 h. Senescent cells were identified as blue-stained cells by standard light microscopy, and a total of 500 cells were counted in five random fields on a slide to determine the percentage of SA-β-gal-positive cells.

Acknowledgments

References

Ahmed-Choudhury, J., Agathanggelou, A., Fenton, S.L., Ricketts, C., Clark, G.J., Maher, E.R., and Latif, F. 2005. Transcriptional regulation of cyclin A2 by RASSF1A through the enhanced binding of p120^{E4F} to the cyclin A2 promoter. *Cancer Res.* **65:** 2690–2697.

Benveniste, P., Cantin, C., Hyam, D., and Iscove, N.N. 2003. Hematopoietic stem cells engraft in mice with absolute efficiency. *Nat. Immunol.* **4:** 708–713.

Borden, K.L., CampbellDwyer, E.J., Carlile, G.W., Djavani, M., and Salvato, M.S. 1998. Two RING finger proteins, the oncoprotein PML and the arenavirus Z protein, colocalize with the nuclear fraction of the ribosomal P proteins. *J. Virol.* **72:** 3819–3826.

Bruggeman, S.W., Valk-Lingbeek, M.E., van der Stoop, P.P., Jacobs, J.J., Kieboom, K., Tanger, E., Hulsman, D., Leung, C., Arsenijevic, Y., Marino, S., et al. 2005. Ink4a and Arf differentially affect cell proliferation and neural stem cell self-renewal in Bmi1-deficient mice. *Genes* & *Dev.* **19:** 1438–1443.

Buchwald, G., van der Stoop, P., Weichenrieder, O., Perrakis, A., van Lohuizen, M., and Sixma, T.K. 2006. Structure and E3-ligase activity of the Ring–Ring complex of Polycomb proteins Bmi1 and Ring1b. *EMBO J.* **25:** 2465–2474.

Cao, R., Tsukada, Y., and Zhang, Y. 2005. Role of Bmi-1 and Ring1A in H2A ubiquitylation and Hox gene silencing. *Mol. Cell* **20:** 845–854.

Core, N., Bel, S., Gaunt, S.J., Aurrand-Lions, M., Pearce, J., Fisher, A., and Djabali, M. 1997. Altered cellular proliferation and mesoderm patterning in Polycomb-M33-deficient mice. *Development* **124:** 721–729.

Fajas, L., Paul, C., Zugasti, O., Le Cam, L., Polanowska, J., Fabbrizio, E., Medema, R., Vignais, M.L., and Sardet, C. 2000. pRB binds to and modulates the transrepressing activity of the E1A-regulated transcription factor p120^{E4F}. *Proc. Natl. Acad. Sci.* **97:** 7738–7743.

Fajas, L., Paul, C., Vie, A., Estrach, S., Medema, R., Blanchard, J.M., Sardet, C., and Vignais, M.L. 2001. Cyclin A is a mediator of p120^{E4F}-dependent cell cycle arrest in G$_1$. *Mol. Cell. Biol.* **21:** 2956–2966.

Fenton, S.L., Dallol, A., Agathanggelou, A., Hesson, L., Ahmed-Choudhury, J., Baksh, S., Sardet, C., Dammann, R., Minna, J.D., Downward, J., et al. 2004. Identification of the E1A-regulated transcription factor p120^{E4F} as an interacting partner of the RASSF1A candidate tumor suppressor gene. *Cancer Res.* **64:** 102–107.

Fernandes, E.R., Zhang, J.Y., and Rooney, R.J. 1998. Adenovirus E1A-regulated transcription factor p120^{E4F} inhibits cell growth and induces the stabilization of the cdk inhibitor p21^{WAF1}. *Mol. Cell. Biol.* **18:** 459–467.

Hernandez-Munoz, I., Lund, A.H., van der Stoop, P., Boutsma, E., Muijrers, I., Verhoeven, E., Nusinow, D.A., Panning, B., Marahrens, Y., and van Lohuizen, M. 2005. Stable X chromosome inactivation involves the PRC1 Polycomb complex and requires histone MACROH2A1 and the CULLIN3/ SPOP ubiquitin E3 ligase. *Proc. Natl. Acad. Sci.* **102:** 7635–7640.

Itahana, K., Zou, Y., Itahana, Y., Martinez, J.L., Beausejour, C., Jacobs, J.J., Van Lohuizen, M., Band, V., Campisi, J., and Dimri, G.P. 2003. Control of the replicative life span of human fibroblasts by p16 and the polycomb protein Bmi-1. *Mol. Cell. Biol.* **23:** 389–401.

Iwama, A., Oguro, H., Negishi, M., Kato, Y., Morita, Y., Tsukui, H., Ema, H., Kamijo, T., Katoh-Fukui, Y., Koseki, H., et al. 2004. Enhanced self-renewal of hematopoietic stem cells

mediated by the Polycomb gene product Bmi-1. *Immunity* **21:** 843–851.

Jacobs, J.J., Kieboom, K., Marino, S., DePinho, R.A., and van Lohuizen, M. 1999. The oncogene and Polycomb-group gene bmi-1 regulates cell proliferation and senescence through the ink4a locus. *Nature* **397:** 164–168.

Kamijo, T., Weber, J.D., Zambetti, G., Zindy, F., Roussel, M.F., and Sherr, C.J. 1998. Functional and physical interactions of the ARF tumor suppressor with p53 and Mdm2. *Proc. Natl. Acad. Sci.* **95:** 8292–8297.

Le Cam, L., Lacroix, M., Ciemerych, M.A., Sardet, C., and Sicinski, P. 2004. The E4F protein is required for mitotic progression during embryonic cell cycles. *Mol. Cell. Biol.* **24:** 6467–6475.

Lessard, J. and Sauvageau, G. 2003. Bmi-1 determines the proliferative capacity of normal and leukaemic stem cells. *Nature* **423:** 255–260.

Lessard, J., Baban, S., and Sauvageau, G. 1998. Stage-specific expression of Polycomb group genes in human bone marrow cells. *Blood* **91:** 1216–1224.

Lessard, J., Schumacher, A., Thorsteinsdottir, U., van Lohuizen, M., Magnuson, T., and Sauvageau, G. 1999. Functional antagonism of the Polycomb-Group genes eed and Bmi1 in hemopoietic cell proliferation. *Genes & Dev.* **13:** 2691–2703.

Miyazaki, M., Kawamoto, H., Kato, Y., Itoi, M., Miyazaki, K., Masuda, K., Tashiro, S., Ishihara, H., Igarashi, K., Amagai, T., et al. 2005. Polycomb group gene mel-18 regulates early T progenitor expansion by maintaining the expression of Hes-1, a target of the Notch pathway. *J. Immunol.* **174:** 2507–2516.

Moehrle, A. and Paro, R. 1994. Spreading the silence: Epigenetic transcriptional regulation during *Drosophila* development. *Dev. Genet.* **15:** 478–484.

Molofsky, A.V., He, S., Bydon, M., Morrison, S.J., and Pardal, R. 2005. Bmi-1 promotes neural stem cell self-renewal and neural development but not mouse growth and survival by repressing the p16^{Ink4a} and p19^{Arf} senescence pathways. *Genes & Dev.* **19:** 1432–1437.

Nolz, J.C., Gomez, T.S., and Billadeau, D.D. 2005. The Ezh2 methyltransferase complex: Actin up in the cytosol. *Trends Cell Biol.* **15:** 514–517.

Ohta, H., Sawada, A., Kim, J.Y., Tokimasa, S., Nishiguchi, S., Humphries, R.K., Hara, J., and Takihara, Y. 2002. Polycomb group gene rae28 is required for sustaining activity of hematopoietic stem cells. *J. Exp. Med.* **195:** 759–770.

Park, I.K., Qian, D., Kiel, M., Becker, M.W., Pihalja, M., Weissman, I.L., Morrison, S.J., and Clarke, M.F. 2003. Bmi-1 is required for maintenance of adult self-renewing haematopoietic stem cells. *Nature* **423:** 302–305.

Pomerantz, J., Schreiber-Agus, N., Liegeois, N.J., Silverman, A., Alland, L., Chin, L., Potes, J., Chen, K., Orlow, I., Lee, H.W., et al. 1998. The Ink4a tumor suppressor gene product, p19^{Arf}, interacts with MDM2 and neutralizes MDM2's inhibition of p53. *Cell* **92:** 713–723.

Quelle, D.E., Zindy, F., Ashmun, R.A., and Sherr, C.J. 1995. Alternative reading frames of the INK4a tumor suppressor gene encode two unrelated proteins capable of inducing cell cycle arrest. *Cell* **83:** 993–1000.

Rooney, R.J. 2001. Cell cycle attenuation by p120^{E4F} is accompanied by increased mitotic dysfunction. *Cell Growth Differ.* **12:** 505–516.

Serrano, M., Hannon, G.J., and Beach, D. 1993. A new regulatory motif in cell-cycle control causing specific inhibition of cyclin D/CDK4. *Nature* **366:** 704–707.

Su, I.H., Dobenecker, M.W., Dickinson, E., Oser, M., Basavaraj, A., Marqueron, R., Viale, A., Reinberg, D., Wulfing, C., and Tarakhovsky, A. 2005. Polycomb group protein ezh2 controls actin polymerization and cell signaling. *Cell* **121:** 425–436.

Tessari, M.A., Gostissa, M., Altamura, S., Sgarra, R., Rustighi, A., Salvagno, C., Caretti, G., Imbriano, C., Mantovani, R., Del Sal, G., et al. 2003. Transcriptional activation of the cyclin A gene by the architectural transcription factor HMGA2. *Mol. Cell. Biol.* **23:** 9104–9116.

Thorsteinsdottir, U., Mamo, A., Kroon, E., Jerome, L., Bijl, J., Lawrence, H.J., Humphries, K., and Sauvageau, G. 2002. Overexpression of the myeloid leukemia-associated Hoxa9 gene in bone marrow cells induces stem cell expansion. *Blood* **99:** 121–129.

Tokimasa, S., Ohta, H., Sawada, A., Matsuda, Y., Kim, J.Y., Nishiguchi, S., Hara, J., and Takihara, Y. 2001. Lack of the Polycomb-group gene rae28 causes maturation arrest at the early B-cell developmental stage. *Exp. Hematol.* **29:** 93–103.

Valk-Lingbeek, M.E., Bruggeman, S.W., and van Lohuizen, M. 2004. Stem cells and cancer; the Polycomb connection. *Cell* **118:** 409–418.

van der Lugt, N.M., Domen, J., Linders, K., van Roon, M., Robanus-Maandag, E., te Riele, H., van der Valk, M., Deschamps, J., Sofroniew, M., van Lohuizen, M., et al. 1994. Posterior transformation, neurological abnormalities, and severe hematopoietic defects in mice with a targeted deletion of the bmi-1 proto-oncogene. *Genes & Dev.* **8:** 757–769.

Voncken, J.W., Schweizer, D., Aagaard, L., Sattler, L., Jantsch, M.F., and van Lohuizen, M. 1999. Chromatin-association of the Polycomb group protein BMI1 is cell cycle-regulated and correlates with its phosphorylation status. *J. Cell Sci.* **112:** 4627–4639.

Voncken, J.W., Niessen, H., Neufeld, B., Rennefahrt, U., Dahlmans, V., Kubben, N., Holzer, B., Ludwig, S., and Rapp, U.R. 2005. MAPKAP kinase 3pK phosphorylates and regulates chromatin association of the Polycomb group protein Bmi1. *J. Biol. Chem.* **280:** 5178–5187.

Wang, H., Wang, L., Erdjument-Bromage, H., Vidal, M., Tempst, P., Jones, R.S., and Zhang, Y. 2004. Role of histone H2A ubiquitination in Polycomb silencing. *Nature* **431:** 873–878.

Weber, J.D., Taylor, L.J., Roussel, M.F., Sherr, C.J., and Bar-Sagi, D. 1999. Nucleolar Arf sequesters Mdm2 and activates p53. *Nat. Cell Biol.* **1:** 20–26.

Zhao, Y., Lin, Y., Zhan, Y., Yang, G., Louie, J., Harrison, D.E., and Anderson, W.F. 2000. Murine hematopoietic stem cell characterization and its regulation in BM transplantation. *Blood* **96:** 3016–3022.